

Combustion synthesis of oxide materials for nuclear waste immobilization

M MUTHURAMAN, N ARUL DHAS and K C PATIL

Department of Inorganic and Physical Chemistry, Indian Institute of Science, Bangalore 560 012, India

Abstract. Oxide materials like perovskite, zirconolite, hollandite, pyrochlore, NASICON and sphene which are used for nuclear waste immobilization have been prepared by a solution combustion process. The process involves the combustion of stoichiometric amount of corresponding metal nitrates and carbonylhydrazide/tetraformyl triazine/diformyl hydrazide at 450°C. The combustion products have been characterized using powder X-ray diffraction, infrared spectroscopy, and ^{29}Si MAS-NMR. The fine particle nature of the combustion derived powders has been studied using density, particle size, BET surface area measurements and scanning electron microscopy. Sintering of combustion derived powder yields 85-95% dense ceramics in the temperature range 1000°-1300°C.

Keywords. Combustion synthesis; SYNROC; nuclear waste immobilization.

1. Introduction

Ceramic oxide materials such as perovskite (CaTiO_3), zirconolite $\text{CaZrTi}_2\text{O}_7$, hollandite ($\text{Ba}_{1.23}\text{Al}_{2.46}\text{Ti}_{5.54}\text{O}_{16}$), pyrochlore ($\text{Ln}_2\text{Zr}_2\text{O}_7$ and $\text{Ln}_2\text{Ti}_2\text{O}_7$, Ln = rare earth metals), NASICON ($\text{Na}_{1+x}\text{Zr}_2\text{P}_{3-x}\text{Si}_x\text{O}_{12}$) and sphene (CaTiSiO_5) have gained tremendous interest because of their application as the geological medium for the immobilization of radioactive wastes (Clarke 1983; Hayward and Cecchetto 1984). The stacking of the metal-oxygen polyhedra in their structure results in the formation of cavities and vacant interlayers capable of accommodating a large number of radioactive cations. The most popular procedure employed by the nuclear power establishments during the past few decades has been to incorporate the nuclear wastes into borosilicate glasses. The serious disadvantage recognized recently is that the borosilicate glasses readily devitrify when subjected to action of water and steam at elevated temperatures and pressure (MacCarthy *et al* 1978). Therefore an alternative method using ceramic materials in which the radionuclides are incorporated into solid solution in an assemblage of mineralogical phases is adopted by several workers (MacCarthy and Davidson 1975; Ringwood *et al* 1979). Since the nuclear waste contains a variety of ions of various sizes and charge, it is difficult to incorporate all the radioactive ions in one phase. So a mixture of phases, i.e. a phase assemblage in which the phases are chemically compatible with one another, has been considered. A variety of phase assemblages have been proposed like supercalcine (MacCarthy 1976; 1979) containing scheelite, cubic zirconia, spinel, apatite, corundum and pollucite phases. Synthetic rock (SYNROC), a titanate based ceramic containing hollandite, perovskite and zirconolite phases, has been investigated (Ringwood *et al* 1979) for nuclear waste immobilization. Fine crystals of sphene (CaTiSiO_5 , calcium titanosilicate) in an aluminosilicate glass matrix are also being

studied as alternatives to glasses for the immobilization of nuclear wastes (Hayward and Cecchetto 1984; Hayward *et al* 1984).

The nuclear applications need highly reactive oxide powders in order to readily assimilate the radioactive nuclei in their structure. The conventional methods (heat and beat, shake and bake) of preparing these materials involve firing the component oxides at elevated temperature with repeated grinding operations to ensure homogeneity. However wet chemical methods (Segal 1989) like sol-gel which have better control over homogeneity, stoichiometry and purity are increasingly used these days for the preparation of sinterable powders. In this paper, we describe the preparation of perovskite (CaTiO_3), zirconolite ($\text{CaZrTi}_2\text{O}_7$), hollandite ($\text{Ba}_{1.23}\text{Al}_{2.46}\text{Ti}_{5.54}\text{O}_{16}$) and sphene (CaTiSiO_5) by solution combustion method. The combustion derived powders have been characterized by powder pattern X-ray diffractometry, IR spectroscopy, BET surface area analysis, particle size measurement, ^{29}Si MAS-NMR, density measurements and scanning electron microscopy.

2. Experimental

2.1 Preparation of titanyl nitrate

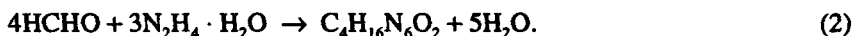
Titanyl nitrate $\text{TiO}(\text{NO}_3)_2$ was prepared by the addition of 1 : 1 ammonia solution to titanyl chloride, TiOCl_2 at 4°C. The resulting hydroxide product was dried and dissolved in a minimum quantity of dilute HNO_3 to get titanyl nitrate. The formation of titanyl nitrate was confirmed by determining the Ti content gravimetrically as TiO_2 (Yamamura *et al* 1985).

2.2 Preparation of fuels

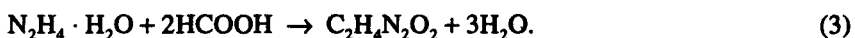
2.2a Preparation of carbohydrazide (CH): Carbohydrazide (CH) $\text{N}_2\text{H}_3\text{CON}_2\text{H}_3$ was prepared as reported (Mohr *et al* 1953) by the hydrazinolysis of diethylcarbonate using hydrazine hydrate (99%)



2.2b Preparation of tetraformyl trisazine (TFTA): Tetraformyl trisazine (TFTA) $\text{C}_4\text{H}_{16}\text{N}_6\text{O}_2$ was prepared by the dropwise addition of 4 mole of formaldehyde to 3 mole of hydrazine hydrate maintaining the temperature below 5°C as reported below (Mashima 1966).



2.2c Preparation of diformyl hydrazide (DFH): N,N'-diformyl hydrazine (DFH) $\text{C}_2\text{H}_4\text{N}_2\text{O}_2$ was prepared by heating 1 : 2 molar ratio of hydrazine hydrate and formic acid on a steam bath overnight. The solvent was removed and ethanol was added. The solid separated was collected and dried (Ainsworth and Jones 1955)



2.3 Calculation of stoichiometry for the combustion reactions

The stoichiometric composition of the redox mixtures for the combustion were calculated using the total oxidizing (O) and reducing (F) valencies of the components which serve as the numerical coefficient for the stoichiometric balance, so that the equivalence ratio Φ_e is unity (i.e. $O/F = 1$) and the energy released by the combustion is maximum (Jain *et al* 1981). Based on the concepts of propellant chemistry the elements C, H, Ca, Ti, Zr, Ba, Al and Si are considered as reducing elements with valencies of 4+, 1+, 2+, 4+, 4+, 2+, 3+ and 4+ respectively and oxygen is an oxidizer having the valency of 2-. The valency of nitrogen is taken as zero because of its conversion to molecular nitrogen during combustion. Accordingly the valencies of $Zr(NO_3)_4$, $TiO(NO_3)_2$, $Ca(NO_3)_2$, $Ba(NO_3)_2$, $Al(NO_3)_3$, CH_6N_4O (CH), $C_4H_{16}N_6O_2$ (TFTA) and $C_2H_4N_2O_2$ (DFH) will be 20-, 10-, 10-, 10-, 15-, 8+, 28+, 8+, respectively. The valency of SiO_2 is zero.

2.3a Synthesis of calcium titanate: Synthesis of calcium titanate ($CaTiO_3$) is described as a representative. Calcium nitrate (5 g), titanyl nitrate (4 g) and TFTA (3 g) were dissolved in minimum amount of water in a pyrex dish. The dish containing the solution was introduced into a muffle furnace maintained at 450°C.

Table 1. Composition of the redox mixtures and the thermal phase evolution of combustion products.

Composition	Compound	Calcination Temp. (°C)	Phases
A (5 g) + B (4 g) + TFTA (2.7 g)	$CaTiO_3$	-	-
A (2 g) + B (3.48 g) + C (3.87 g) + CH (4.76 g)	$CaZrTi_2O_7$	As prepared 700 900 1000	TiO_2 (a) + ZrO_2 (t) TiO_2 (r) + ZrO_2 (r) + $CaTiO_3$ + $CaZrTi_2O_7$ TiO_2 (r) + $CaZrTi_2O_7$ $CaZrTi_2O_7$
D (1 g) + B (3.24 g) + E (2.9 g) + CH (3.7 g)	Hollandite	As prepared 1000	Amorphous Hollandite
A (1.84 g) + B (4.7 g) + C (1.02 g) + D (0.52 g) + E (2.48 g) + CH (2 g) + TFTA (2.1 g)	SYNROC	As prepared 1100	Amorphous + perovskite Perovskite + Zirconolite + Hollandite
A (6.83 g) + B (5.43 g) + F (1.47 g) + CH (6.5 g)	$CaTiSiO_5$	As prepared 400 600 800 875 950 1200	Amorphous + CaO + TiO_2 (r) CaO + TiO_2 + $CaTiO_3$ $CaTiO_3$ + CaO + TiO_2 $CaTiSiO_5$ + $CaTiO_3$ + SiO_2 $CaTiSiO_5$ + $CaTiO_3$ + SiO_2 $CaTiSiO_5$ + $CaTiO_3$ + SiO_2 $CaTiSiO_5$
A (4.53 g) + B (3.6 g) + F (1.15 g) + TFTA (2.5 g)	$CaTiSiO_5$	1250	$CaTiSiO_5$
A (4.84 g) + B (3.85 g) + F (1.23 g) + DFH (9G)	$CaTiSiO_5$	1200	$CaTiSiO_5$

A = $Ca(NO_3)_2$, B = $TiO(NO_3)_2$, C = $Zr(NO_3)_4$, D = $Ba(NO_3)_2$, E = $Al(NO_3)_3$, F = Fumed SiO_2 , CH = carbonylhydrazide, TFTA = tetraformyl trisazine, DFH = diformyl hydrazide.

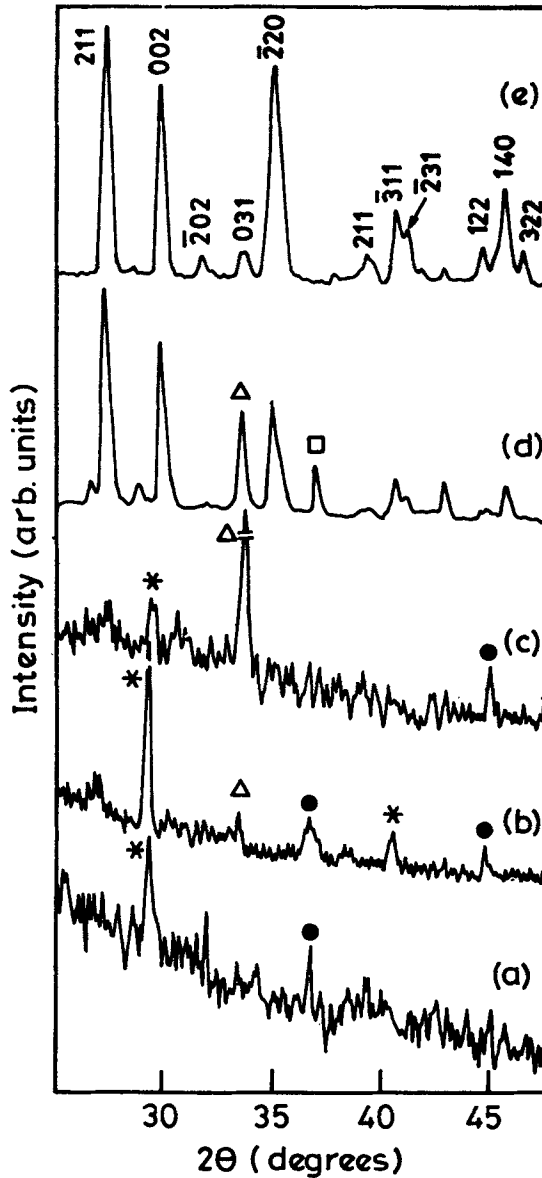


Figure 1. X-ray diffraction patterns of sphene: (a) as prepared, (b) 400°C, (c) 600°C, (d) 875°C and (e) 1200°C. (*, CaO; ●, TiO₂; Δ, CaTiO₃; □, α -crystalbite).

The solution undergoes dehydration followed by decomposition with the evolution of large amount of gases (oxides of nitrogen and ammonia) and ignites to burn with a flame (flame temperature, $900 \pm 50^\circ\text{C}$) yielding voluminous calcium titanate powder in less than 5 min.

Similarly calcium zirconolite, hollandite, SYNROC and sphene (using three different fuels) were prepared using combustion process. Actual compositions of the redox mixture used for the combustion are summarized in table 1.

Table 2. The lattice parameters of the combustion products.

Compound	a (Å)	b (Å)	c (Å)	α (°)	β (°)	γ (°)
CaTiO ₃	5.4138	7.6573	5.3840	90	90	90
CaZrTi ₂ O ₇	12.4412	7.2151	11.50332	90	100.28	90
Hollandite	9.902	9.902	2.865	90	90	90
CaTiSiO ₅ /CH	6.975	8.7175	6.5107	90	113.22	90
CaTiSiO ₅ /TFTA	7.0321	8.7167	6.5508	90	113.69	90
CaTiSiO ₅ /DFH	7.0526	8.6969	6.5612	90	113.93	90

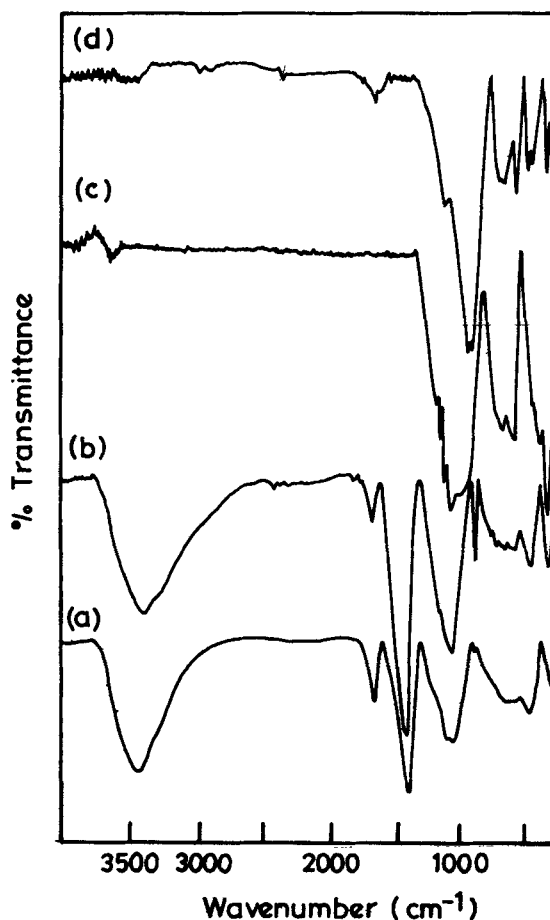


Figure 2. IR spectra of sphene; (a) as prepared, (b) 400°C, (c) 700°C and (d) 1100°C.

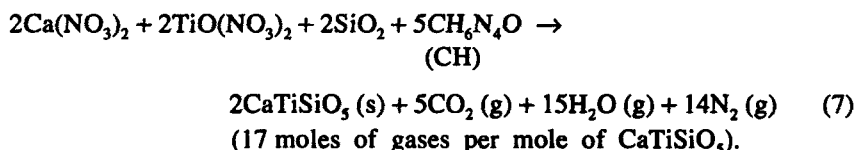
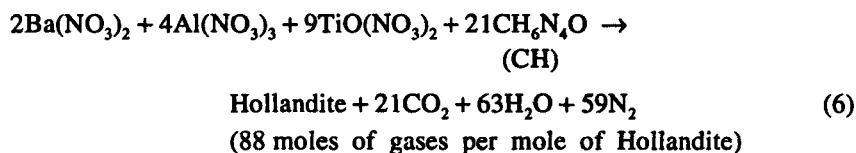
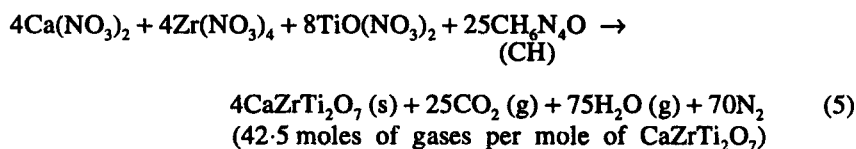
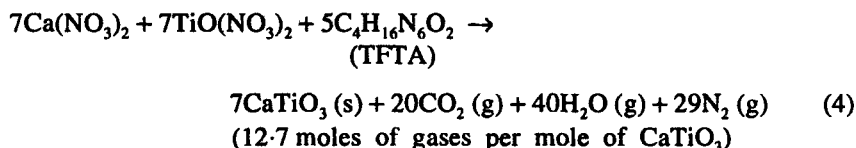
2.3b Product analysis: The combustion derived products have been characterized by powder XRD, recorded using Philips PW 1050/70 X-ray diffractometer with Ni-filtered Cu-K α radiation. Lattice parameters were calculated from XRD pattern in the range of $25^\circ \leq 2\theta \leq 55^\circ$ with a least-squares fit. The IR spectra were

obtained using BIO-RAD SKC 3200 FT-IR Spectrometer as KBr pellets. High resolution ^{29}Si MAS-NMR spectra of combustion products were recorded using Bruker MSL-300 spectrometer (Switzerland, SPECTROSPIN AG). A centrifugal photo sedimentation method (Model SKC 2000 Micron photosizer) was used to determine the agglomerate particle size (i.e., Stokes diameter) and distribution of the particles (histogram). Surface areas were measured using nitrogen gas adsorption multi-point BET method (Model 2100E Accusorb, Micromeritics Instrument Corp., Norcross, GA) assuming a cross sectional area of 0.162 nm^2 for the nitrogen molecule. The powder densities were measured using a pycnometer with xylene as liquid medium.

The combustion derived products were crushed and cold-pressed under 50 MPa uniaxial pressure. The resulting green bodies have 40–50% theoretical density. Sintering of cold-pressed compacts were carried out by heating the specimens at desired temperatures in air. The bulk density of the sintered pellets were measured using Archimedes liquid displacement technique. Microstructure of sintered pellets were studied using a scanning electron microscope (SEM, Model S-150 Stereoscan, Cambridge Physical Sciences, Cambridge, UK).

3. Results and discussion

Formation of calcium titanate, calcium zirconolite, hollandite and calcium titanosilicates by the combustion reactions may be written as:



The solid product of combustion have been identified by their characteristic

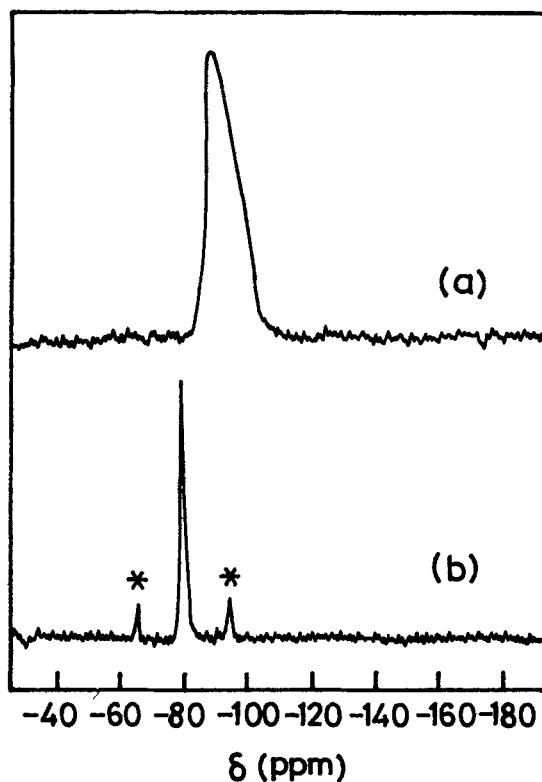


Figure 3. ^{29}Si MAS-NMR of sphene: (a) as prepared and (b) 1100°C.

Table 3. The particulate properties of the combustion products.

Compound	Powder density (g/cm ³)	Surface area (m ² /g)	50% Average agglomerated particle size (μm)	Particle size ^a (μm)	Ref
Ln ₂ Zr ₂ O ₇	4.1	14	1.08	0.10	Arul Dhas and Patil (1993)
NASICONs	2.4–2.8	8–30	6–13	–	Arul Dhas and Patil (1994)
CaTiO ₃	3.46	21	0.91	0.08	present study
CaZrTi ₂ O ₇	2.8	39	9.3	0.05	present study
Hollandite	3.94	37	11.5	0.04	present study
SYNROC	4.98	9	3.6	0.13	present study
Sphene/CH	2.57	67	9.0	0.03	present study
Sphene/TFTA	2.83	65	8.3	0.03	present study
Sphene/DFH	2.9	46	5.7	0.04	present study

a = calculated from surface area measurement (Irani and Callis 1963).

XRD patterns (JCPDS card: CaTiO₃; No. 22-153, CaZrTi₂O₇; No. 34-167, Ba_{1.23}Al_{2.46}Ti_{5.54}O₁₆; No. 33-133, CaTiSiO₅; No. 25-177). Powder XRD patterns of combustion derived sphene (CH process) are shown in figure 1. The as-synthesized residue is X-ray amorphous and shows the presence of weakly crystalline CaO

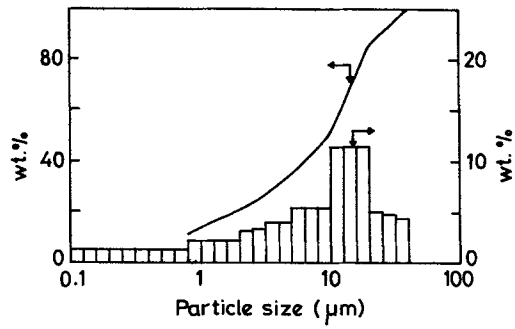
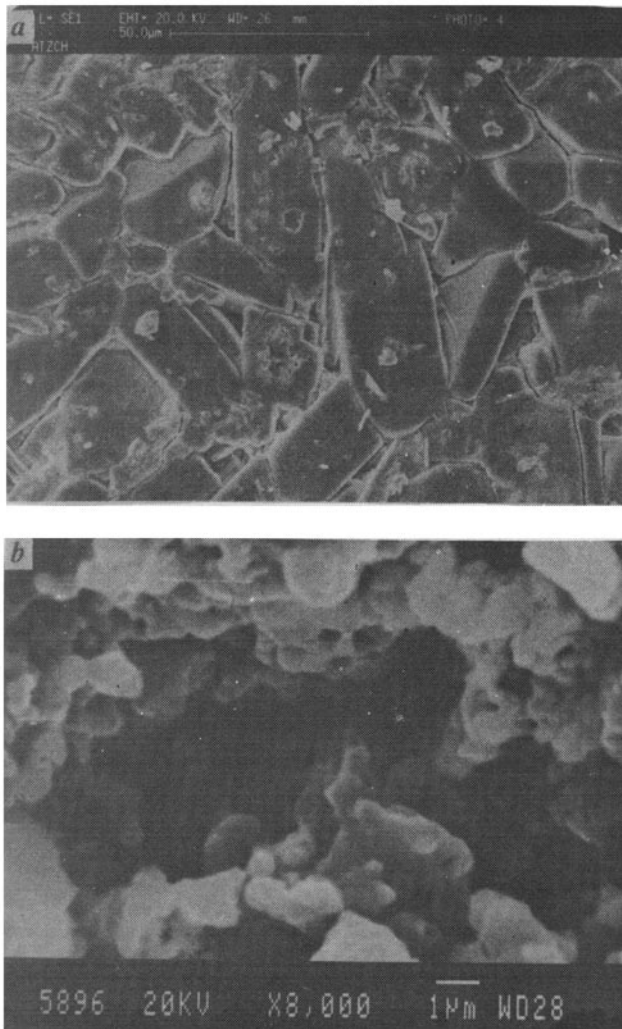


Figure 4. Particle size distribution of combustion derived zirconolite.



Figures 5a, b. For caption, see p. 985.

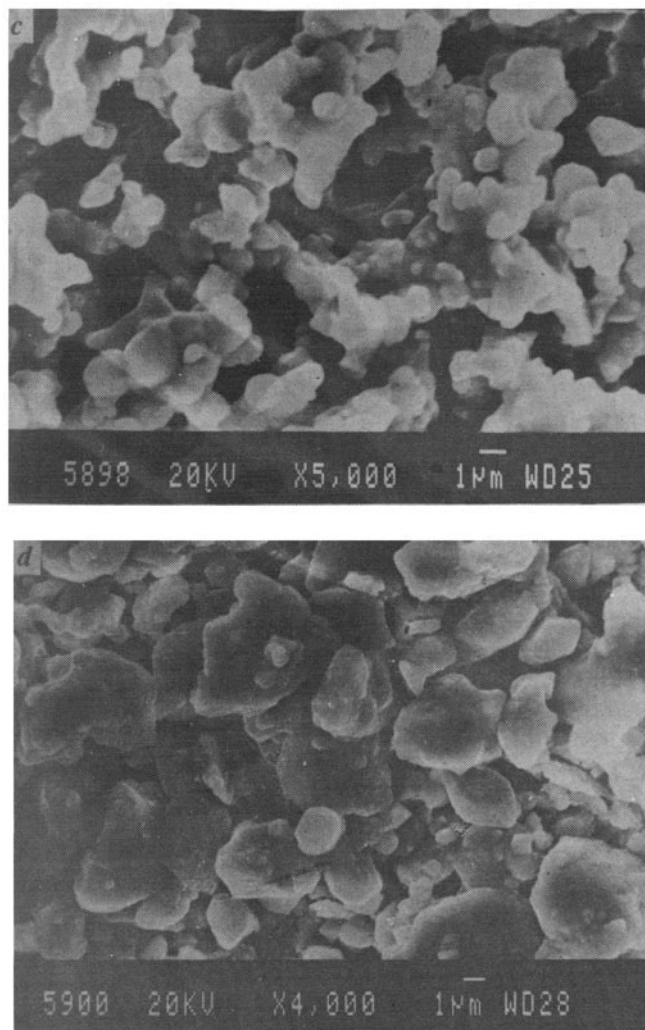


Figure 5. a–d. SEM microstructures; (a) zirconolite sintered at 1250°C, (b) sphene sintered at 1100°C, (c) sphene sintered at 1200°C and (d) sphene sintered at 1300°C.

(figure 1a). At 600°C calcium titanate is the major phase along with CaO and TiO₂ (figure 1c). On further increase in the calcination temperature CaTiO₃, CaO and TiO₂ appear to react with SiO₂ to form CaTiSiO₅. α -crystoballite emerges out as a secondary intermediate phase (figure 1d) between 850°C and 1000°C as reported (Chen *et al* 1994). As the formation of CaTiSiO₅ progresses the amount of CaTiO₃ and SiO₂ decreases. The lattice parameters calculated with a least squares-fit using XRD reflections are given in table 2. These values are in good agreement with those reported in literature.

Various intermediate phases formed during the calcination are summarized in table 1. Powder XRD pattern of as-synthesized zirconolite showed the presence of

TiO₂ (anatase) and tetragonal ZrO₂. At 700°C TiO₂, ZrO₂ and CaTiO₃ phases are observed along with a small amount of zirconolite. On further increase in the calcination temperature CaTiO₃ appears to react with TiO₂ and ZrO₂ to form zirconolite. The formation of single phase zirconolite occurred at 1000°C. The relatively low formation temperature (1000–1200°C) of zirconolite, hollandite and sphene indicates the high reactivity of combustion products.

The IR spectra of combustion derived sphene are shown in figure 2. The IR spectra show the characteristic absorption of SiO₄ tetrahedra at 560 and 880 cm⁻¹ (figure 2d). The absorption band around 675 cm⁻¹ is assigned to TiO₆ octahedra (Chen and Liu 1994). It is noted that the combustion derived sphene shows broad band around 3415 and 1640 cm⁻¹ which corresponds to O–H stretching and bending vibrations and a sharp absorption band around 1380 cm⁻¹ due to NO₃ stretching (figure 2a). The intensities of these three absorption bands decrease gradually on heating the sample to higher temperature. When the sample is heated above 600°C the absorption bands corresponding to the impurities completely disappear (figure 2c). The occurrence of impurities, such as NO₃ and OH in the combustion synthesized sphene could be due to the presence of fumed SiO₂ in the redox mixture which reduces the flame temperature thereby giving undecomposed products.

The ²⁹Si MAS-NMR of as prepared sphene by CH process shows a broad resonance at -110 ppm (figure 3a) and corresponds to amorphous silica (Macial and Sindorf 1980). The ²⁹Si NMR of heat-treated sphene at 1100°C for 1 h shows a sharp resonance at -80 ppm (figure 3b) consistent with SiO₄ tetrahedra (Lippmaa *et al* 1980). This is a low field shift compared with the resonance frequency of pure SiO₂ which confirms the formation of single phase sphene.

The particulate properties of the combustion derived oxide materials used for nuclear waste immobilization are summarized in table 3. The powder densities of the combustion products range from 60–75% of the theoretical value which indicate the porous nature of the combustion residue. The high surface area of the combustion derived products ranges from 8–67 m²/g and this could be attributed to the large amount of gases evolved during combustion [(4)–(7)] which dissipate the heat thereby inhibiting sintering of the combustion products. The 50% average agglomerated particle size of the combustion derived materials ranges from 0.9–13 μm. As a representation the particle size distribution of zirconolite powder is shown in figure 4. It shows that 60% of the particles are distributed between 10 and 13 μm range with the average agglomerated particle size of 9.3 μm.

The SEM microstructure of sintered zirconolite (1250°C) is shown in figure 5a. The SEM micrograph exhibits the presence of dense elongated grains with linear grain boundaries. The grain size vary from 40–50 μm. The microstructural development of sintered sphene compacts (1100°–1300°C) is illustrated in figures 5b–d. The SEM microstructure of sintered body (1100°C) shows poor densification (63% theoretical density) and the presence of platelet particles with large pores and cavities. When the sintering temperature is increased to 1200°C, the sintered body exhibits a network of nearly equiaxial grains with the homogeneous distribution of pores. The sintered (1300°C) sphene compact shows almost pore free state with the irregular shaped grains (figure 5d). The grains are not well connected and the grain size ranges from 1–5 μm. The sintered body achieves more than 85% theoretical density. Sintering of sphene above 1300°C leads to melting of sphene which eventually reduces the sintered density. The lower sintering temperature of combustion

derived zirconolite and sphene could be due to the large surface area and the fine particle nature of the combustion products.

4. Conclusion

The solution combustion process has been used successfully to prepare reactive oxide materials, which can be used for nuclear waste immobilization. The sintering of sphene and zirconolite compacts in the temperature range of 1250° and 1300°C for 1 h results in a dense body (85–95% theoretical density). SEM of the sintered compacts of sphene showed the presence of almost equiaxial grains of 1–5 µm size and that of zirconolite showed the presence of elongated grains of 40–50 µm size.

References

- Ainsworth C and Jones R G 1955 *J. Am. Chem. Soc.* **77** 621
Arul Dhas N and Patil K C 1993 *J. Mater. Chem.* **3** 1289
Arul Dhas N and Patil K C 1994 *J. Mater. Chem.* **4** 491
Chen S K and Liu H S 1994 *J. Mater. Sci.* **29** 2921
Clarke D R 1983 *Ann. Rev. Mater. Sci.* **13** 191
Hayward P J and Cecchetto E V 1984 in *Scientific basis for nuclear waste management* (ed) Z Lutze (New York: Elsevier) Vol. 5, p. 91
Hayward P J, Vance E R, Cann C D and Mitchell S L 1984 in *Advances in ceramics* (ed) G G Wicks and W A Ross (Ohio: American Ceramic Society, Columbus) Vol 8, p. 291
Irani R R and Callis C F 1963 in *Particle size: measurement, interpretation and application* (New York: John Wiley) p. 125
Jain S R, Adiga K C and Pai Verneker V R 1981 *Combust. Flame* **40** 71
Lippmaa E, Magi M, Samoson A, Engelhardt G and Grimmer A R 1980 *J. Am. Chem. Soc.* **102** 4889
MacCarthy G J 1976 *Trans. Am. Nucl. Soc.* **23** 168
MacCarthy G J 1979 in *Scientific basis for nuclear waste management* (ed) MacCarthy G J (New York: Plenum) Vol. 1, p. 329
MacCarthy G J and Davidson M T 1975 *Am. Ceram. Soc. Bull.* **54** 782
MacCarthy G J, White W B, Rustum Roy, Scheetz B E, Komarneni S, Smith D K and Roy D M 1978 *Nature (London)* **273** 216
Macial G and Sindorf D 1980 *J. Am. Chem. Soc.* **102** 7606
Mashima M 1966 *Bull. Chem. Soc. Jpn.* **39** 504
Mohr E B, Brezinski J J and Audrieth L F 1953 *Inorg. Synth.* **4** 32
Ringwood A E, Kesson S E, Ware N G, Hibberson W and Major A 1979 *Nature (London)* **278** 219
Segal D 1989 *Chemical synthesis of advanced ceramic materials* (Cambridge: Cambridge University Press)
Yamamura H, Tanada M, Tanada H, Shirasaki S and Moriyoshi Y 1985 *Ceram. Int.* **11** 17